Electrical and optical characteristics of the radio frequency surface dielectric barrier discharge plasma actuation*

Wei-Long Wang(王蔚龙), Hui-Min Song(宋慧敏)†, Jun Li(李军), Min Jia(贾敏), Yun Wu(吴云), and Di Jin(金迪)

Science and Technology on Plasma Dynamics Laboratory, Air Force Engineering University, Xi'an 710038, *China*

(Received 19 October 2015; revised manuscript received 3 December 2015; published online 20 February 2016)

Electrical characteristics and optical emission spectrum of the radio frequency (RF) surface dielectric barrier discharge (SDBD) plasma actuation are investigated experimentally in this paper. Influences of operating pressure, duty cycle and load power on the discharge are analyzed. When the operating pressure reaches 30 kPa, the discharge energy calculated from the Charge–Voltage (Q–V) Lissajous figure increases significantly, while the effective capacitance decreases remarkably. As the duty cycle of the applied voltage increases, the voltage–current waveforms, the area of Q–V loop and the capacity show no distinct changes. Below 40 W, effective capacitance increases with the increase of load power, but it almost remains unchanged when load power is between 40 W and 95 W. The relative intensity $I_{391.4}^{\text{peak}}/I_{380.5}^{\text{peak}}$ changes little as the operating pressure varies from 4 kPa to 100 kPa, while it rises evidently with the pressure below 4 kPa, which indicates that the RF discharge mode shifts from filamentary discharge to glow discharge at around 4 kPa. With the increase of load power, the relative intensity $I_{391.4}^{\text{peak}}/I_{380.5}^{\text{peak}}$ rises evidently. Additionally, the relative intensity $I_{371.1}^{\text{peak}}/I_{380.5}^{\text{peak}}$ is insensitive to the pressure, the duty cycle, and the load power.

Keywords: radio frequency discharge, optical emission spectroscopy, charge–voltage Lissajous figure, plasma aerodynamic actuation

PACS: 52.50.Qt, 52.80.Mg, 47.80Jk **DOI:** 10.1088/1674-1056/25/4/045203

1. Introduction

Plasma flow control, based on plasma aerodynamic actuation, is an innovative active flow control technology for improving the aerodynamic performance of aircraft.[1–4]

In order to enhance the flow control ability of the dielectric barrier discharge (DBD) actuator, different plasma sources are adopted and studied, such as AC power supply in dozens of kHz[3,4] and the nanosecond pulsed power supply.[5,6] Wu *et al.*[4] tested emission spectrum characteristics with AC power supply, and found that the rotational temperature increases with the increases of the inner space of an electrode pair. Jiang *et al.* presented two kinds of discharge Lissajous figures in nanosecond-pulse surface discharges. The first Lissajous figure is almond-like, and the other one is like a parallelogram.[6] Dedrick *et al.* investigated the RF plasma propagation of surface barrier discharge in atmospheric pressure air. Experimental results showed that the mean propagation length varied linearly with applied voltage.[7]

Compared with the AC power supply in dozens of kHz and the nanosecond pulsed power supply, RF DBD has advantages such as stable volume discharge in high-speed airflow, high energy coupling efficiency to the ionized gas, etc. Therefore, it has received increasing attention for its promising application in flow control.[8–11] Leonov *et al.*[8] revealed the specific regime of filamentary RF discharge plasma in supersonic airflow. It was found that the temperature of the filamentary RF plasma reached as high as 4000 K at a static pressure of 120 Torr (1 Torr = 1.33322×10^2 Pa). The influence of RF discharge plasma filaments on shock position and amplitude is acquired.[8,9] At the critical attack angle $\alpha = 13^\circ$ of the wing model, through increasing frequency modulation, modulated RF DBD can reduce the drag coefficient by 40%.[10] Dedrick *et al.* investigated a dual-frequency driven plasma actuator, and changed the position of RF 13.56 MHz pulses in the period of a low-frequency 5-kHz sinusoidal voltage. The results show that the optical emission, which is studied by fast imaging is most intense when the pulses are positioned close to the zero crossings of the lower frequency waveform during the positive half-period.[12] However, the connection between the discharge characteristics and some key parameters, such as duty cycle and load power, remains unclear. The understanding of RF surface discharge at low pressure is still insufficient.

In this paper, the electrical characteristics and the optical emission spectrum of the RF surface dielectric barrier discharge (SDBD) are investigated. The influences of operating pressure, duty cycle and load power on RF DBD performance are analyzed.

*Project supported by the National Natural Science Foundation of China (Grant Nos. 11472306, 51276197, and 51336011).

†Corresponding author. E-mail: min_cargi@sina.com

© 2016 Chinese Physical Society and IOP Publishing Ltd

2. Experimental setup

The schematic diagrams of the experiment setup and actuator are shown in Fig. 1(a). The actuator is operated in a pressurized chamber, in which the ambient pressure can be adjusted from 200 Pa to 100 kPa, with environmental temperature of about 300 K. An RF generator/amplifier (AG 1017L, T&C) is used for the discharge, and its output power increases nonlinearly from 0 W to 200 W. The operating frequency varies from 10 kHz to 10 MHz. In the burst mode, the pulse width ranges between 1 μs and 500 μs, and the pulse period changes from 1ms to 50 ms. A transformer matching circuit is designed to elevate the applied voltage and realize the impedance matching between the RF generator and the plasma actuator. The plasma actuator consists of a dielectric barrier and two identical electrodes as shown in Fig. 1(b). The dielectric barrier is made of a 1-mm-thick ceramic plate with a relative permittivity of 9.5. The electrode is 54 mm in length and 2 mm in width, and its material is nickel plated tungsten. The electrodes are separated by a ceramic dielectric barrier with an electrode gap of 1 mm. Inside the pressurized chamber, the actuator is placed 2 cm away from the quartz optical window.

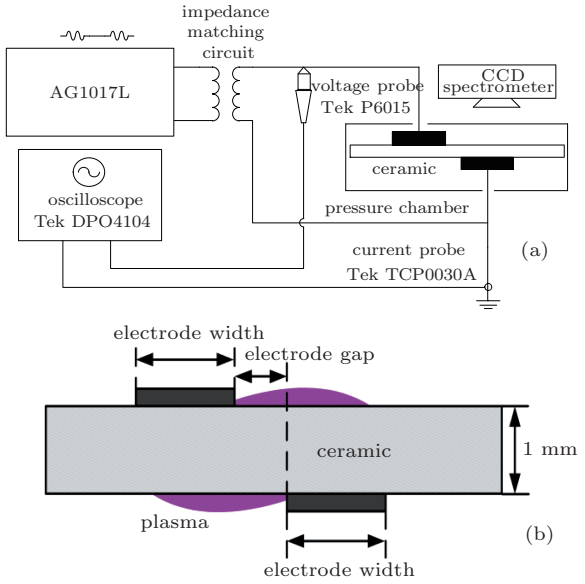


Fig. 1. (color online) Schematic diagrams of the experiment: (a) experimental setup, (b) schematic diagram of the plasma actuator.

The applied voltage and the discharge current are measured with a high voltage probe (Tektronix, P6015A) and a current probe (Tektronix, TCP0030A). All the signals are displayed and recorded by a digital oscilloscope (Tektronix, DPO4104). The optical emission spectra of the RF discharge plasma are obtained with a charge coupled device spectrometer (Avaspec-2048-M), which is outside the pressurized chamber. The head of the optical fiber is 5 mm away from the quartz glass window. The resolution ratio of the spectrometer is no bigger than 0.08 nm and the wavelength ranges from 200 nm to 1000 nm. The emission intensity is averaged temporally and spatially.

3. Results and discussion

3.1. Electrical characteristics

In order to obtain the influences of operating pressure, duty cycle and load power on RF discharge, voltage–current waveforms are recorded under various conditions. The effects of these parameters on discharge energy and capacitance are also investigated by Q–V loops.

3.1.1. Influence of operating pressure on electric characteristics

Figure 2 shows the voltage–current waveforms and images of RF discharge under different operating pressures (1 kPa–100 kPa). The experimental conditions are as follows: the frequency of the RF generator is 0.67 MHz, the duty cycle is 1:20, and the load power is 95 W. As the pressure varies between 1 kPa and 30 kPa, it is found that the current waves have two obvious peaks, and the current spikes increase remarkably as operating pressure rises from 40 kPa to 100 kPa. The discharge voltage becomes bigger when the pressure is relatively higher.

As shown in Fig. 2(a), the glow discharge is uniform and diffuses under lower pressure. From Fig. 2(b) to Fig. 2(f), it is seen that with the increase of pressure, the RF discharge plasmas are focused in several inhomogeneous micro-discharge channels, which are like some diffuse discharge jets. Instead, when operating pressure exceeds 40 kPa, many bright filaments are observed in the image, and also the number of micro-discharge channels increases with the increase of current. Under higher pressure, the air density is higher, which indicates that more molecules are within the same volume, and severer conflict can be acquired. That explains the formation of brighter micro-discharge channels.

An SDBD parallelogram-shape Q–V Lissajous curve which is driven by an AC power generator is shown in Fig. 3.[13–16] The parallelogram corresponds to the change of a discharge period, and the process of A–B corresponds to the so-called dark period[13] where no discharge occurs. The slope of this process quantifies the electrical pure passive-component capacitance of the plasma actuator, which is denoted as C_0.[15] The value of C_0 can be measured by a conventional circuit analyzer, and the result is the same as the slope of A–B. The process of B–C is called the active phase, the effective capacitance C_{eff}[15] can be acquired with the slope of it, which indicates the combination of the passive-component C_0 and the contribution of the plasma itself to the capacitance. It is important to note that C_{eff} provides a quantity for determining the virtual capacitance of the operative plasma actuator. Both of C_0 and C_{eff} should be taken into account for the impedance matching desired in the experiment.

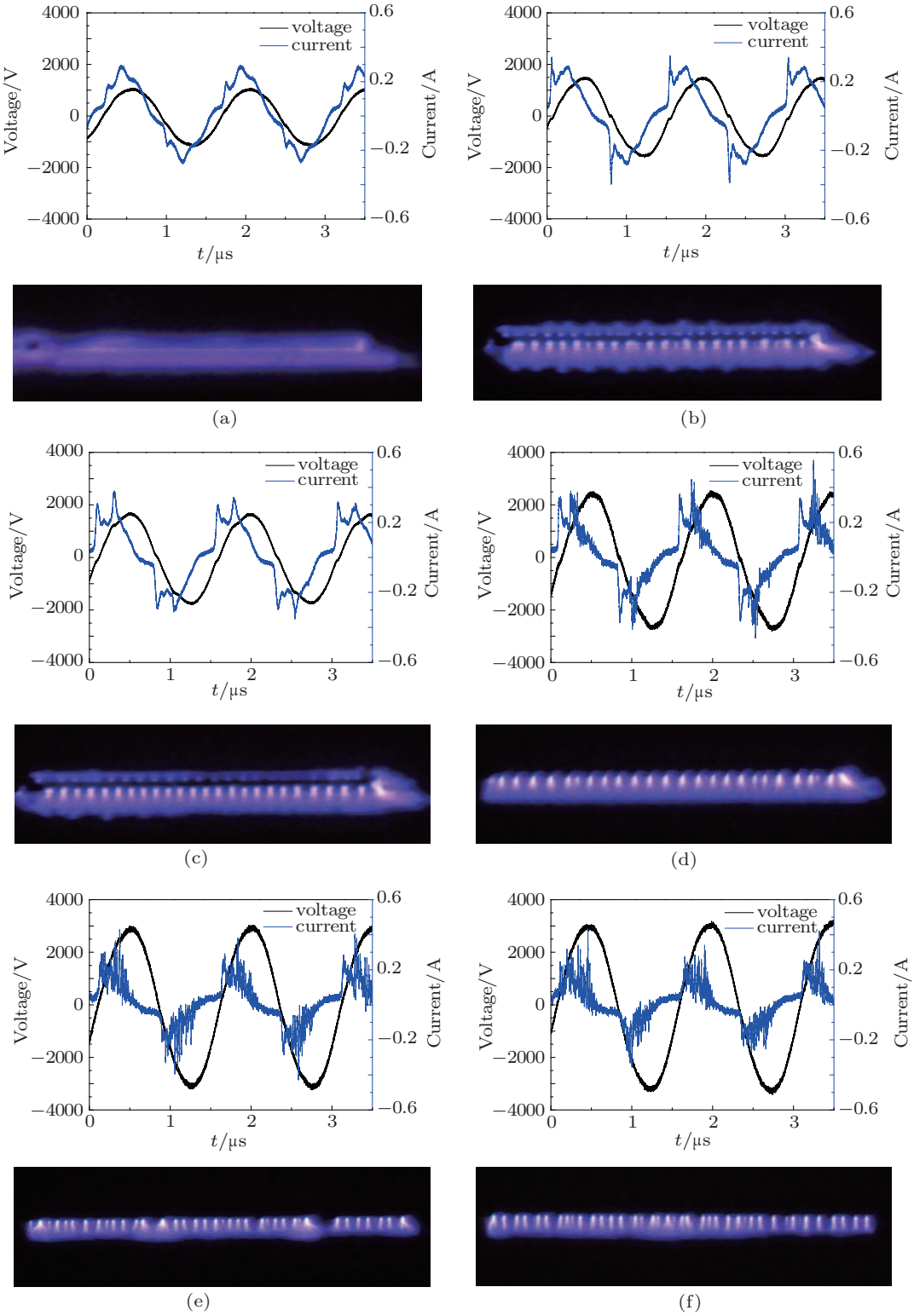


Fig. 2. (color online) The voltage–current waveforms and images of RF discharge under different operating pressures: (a) 1 kPa, (b) 8 kPa, (c) 30 kPa, (d) 40 kPa, (e) 70 kPa, and (f) 100 kPa. In this figure, we take frequency: 0.67 MHz, duty cycle: 1:20, load power: 95 W.

The area of the Q–V Lissajous loop is equal to the energy per cycle, which can be calculated from

$$E = \int Q \cdot \mathrm{d}V = A_{\mathrm{Lissajous}}. \tag{1}$$

At different pressures the shapes of Q–V loops are similar to the parallelogram, as shown in Fig. 4(a). Keeping the duty cycle and load power fixed, the energy per cycle, which is calculated by the area of the loop, is approximately unchanged when the operating pressure varies from 0.6 kPa to 30 kPa. When the operating pressure reaches 30 kPa, the area of the Q–V loop increases significantly. There are three lines plotted in Fig. 4(b) to analyze the capacitance and energy per cycle at different pressures. When the pressure is below 30 kPa, C_{eff} and the energy per cycle show little difference. As the oper-

ating pressure varies from 30 kPa to 40 kPa, $C_{\rm eff}$ decreases remarkably while the energy per cycle increases rapidly with the augment of pressure. Additionally, $C_{\rm eff}$ and energy per cycle change slightly as the operating pressure rises from 40 kPa to 100 kPa. The value of C_0 is insensitive to the pressure, from which it can be concluded that the value of C_0 represents the constant capacitance of the plasma actuator. As pressure rises, the discharge changes from glow mode to filament mode. According to the discharge pictures in Fig. 2, it can be seen that the area of the plasma decreases, which equals the area of $C_{\rm eff}$. Since the capacitance of $C_{\rm eff}$ is proportional to the area of $C_{\rm eff}$, it becomes smaller as shown in Fig. 4(b).

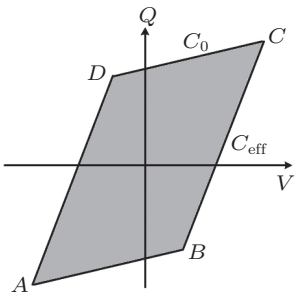


Fig. 3. (color online) Schematic presentation of SDBD Q–V Lissajous figure.[13]

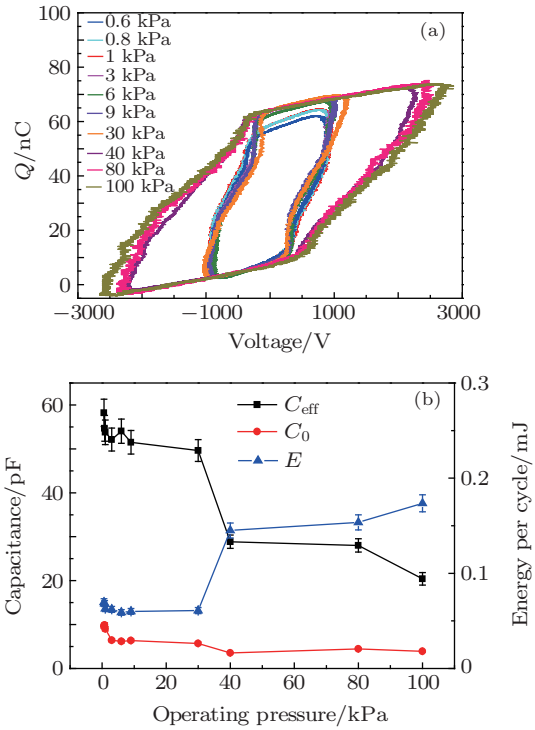


Fig. 4. (color online) Lissajous figures of RF discharge at different pressures: (a) Q–V Lissajous figures at different pressures, (b) capacitance and energy per cycle at different pressures. Other parameters are frequency: 0.67 MHz, duty cycle: 1:20, load power: 95 W.

3.1.2. Influence of duty cycle on electric characteristics

$T_{\rm A}/T_{\rm M}$ is defined as the duty cycle of an RF generator, where $T_{\rm A}$ is burst width, $T_{\rm M}$ is the burst period, and T is the period of voltage waveform. Keeping operating pressure at 50 kPa and power at 95 W, modulating the duty cycles of the RF generator to be 1:5 and 1:20, the voltage–current waveforms and images are shown in Figs. 5(a) and 4(b), which represent the voltage–current waveforms with duty cycles of 1:5 and 1:20, respectively. The peak–peak voltage on the voltage–current plot has no evident change as the duty cycle varies. As shown in Figs. 5(a) and 5(b), the intensity of the RF discharge increases with the ascending of the duty cycle. The single period voltage–current plot of the RF generator is shown in Fig. 5(c), it can be concluded that the duty cycle has little effect on voltage–current waveforms of a period and discharge mode.

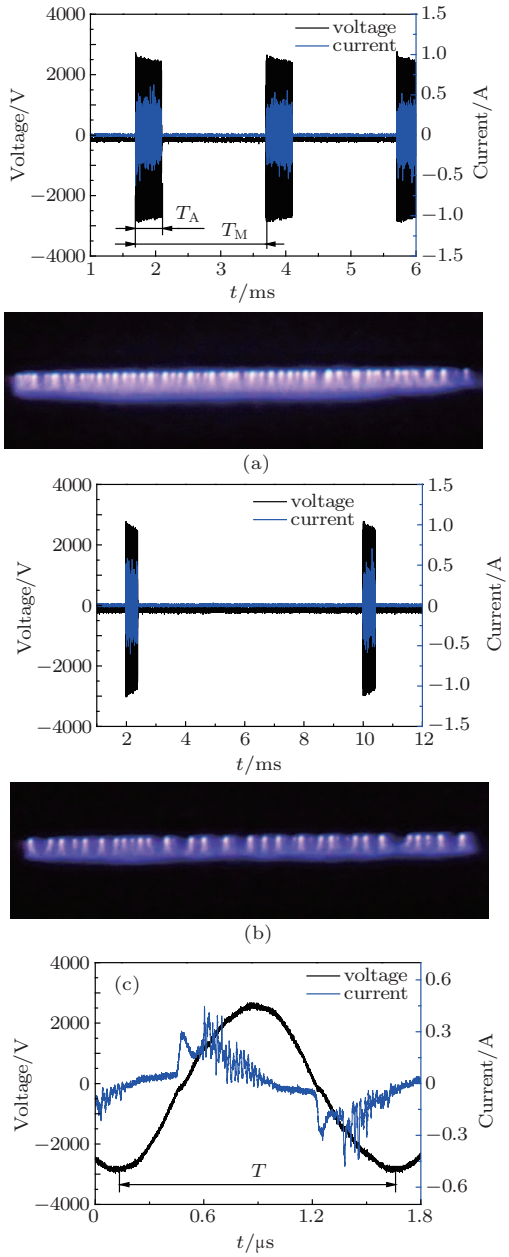


Fig. 5. (color online) Voltage–current waveforms and images of RF discharge under different duty cycles: (a) 1:5, (b) 1:20, and (c) the voltage–current waveforms of a period. Other parameters are frequency: 0.67 MHz, operating pressure: 50 kPa, load power: 95 W.

Figure 6 shows the influences of duty cycle on the Lissajous figure and discharge energy. With the decrease of duty cycle, there is no obvious variation of the Q–V Lissajous loop

as shown in Fig. 6(a). Besides, the plot of $C_{\rm eff}$, C_0, and energy per cycle in Fig. 6(b) are almost unchanged with the decrease of duty cycle, and it also shows that the duty cycle has little effect on the characteristics in the single voltage period.

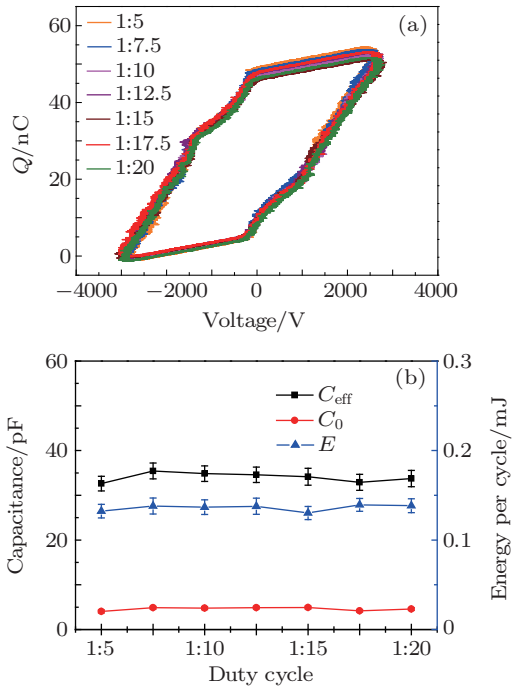


Fig. 6. (color online) Lissajous figures of RF discharge at different duty cycles: (a) Q–V Lissajous figures at different duty cycles, (b) capacitance and energy per cycle at different duty cycles. Other parameters are frequency: 0.67 MHz, operating pressure: 50 kPa, load power: 95 W.

In the burst period, the variation of the duty cycle only changes the duration of the blank output ($T_{\rm A} - T_{\rm M}$), while $T_{\rm A}$ (the period T is multiplied by the pulse number) remains unchanged. In a discharge period, the Lissajous figure is determined by voltage–current waveform, and the capacitance and energy per cycle are calculated by the Lissajous figure. Since the voltage–current waveforms are fixed under different duty cycles, the shapes of the Lissajous figures are almost the same. Obviously the electrical characteristic, including the capacitance and energy per cycle, is changeless under different duty cycles.

3.1.3. Influence of power on electric characteristics

The influence of load power on RF SDBD is studied with the load power ranging from 5 W to 95 W. Figure 7 presents voltage–current waveforms and images of RF discharge under different load powers (21 W and 65 W). The experimental conditions are as follows: the frequency of the RF generator is 0.67 MHz, the operating pressure is 30 kPa, and the duty cycle is 1:20. As shown in Fig. 7, when the load power is 21 W, the current has only one peak; as the load power increases to 65 W, two current peaks are observed. What is more, the peak-to-peak value of the voltage ascends when the power is relatively high. It is found that micro-discharge channels of RF discharge increase remarkably with the increase of load power, which indicates that it is difficult to discharge at lower load power.

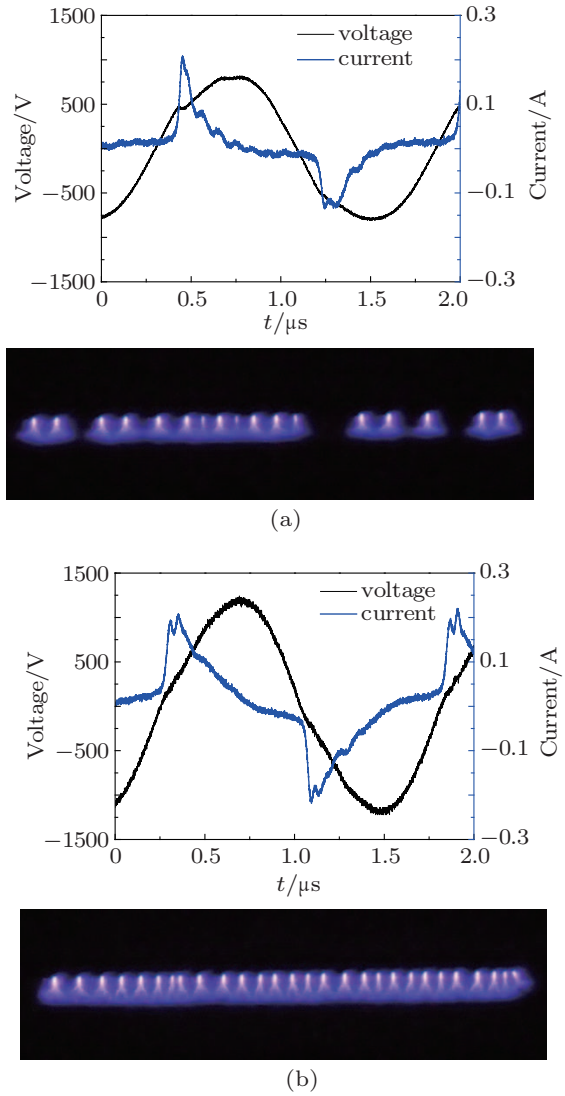


Fig. 7. (color online) Voltage–current waveforms and images of RF discharge under different load powers: (a) 21 W, (b) 65 W. Other parameters are frequency: 0.67 MHz, operating pressure: 30 kPa, duty cycle: 1:20.

Figure 8 presents the Q–V Lissajous figures, capacitance, and energy per cycle at different load powers. As shown in Fig. 8(a), with the increase of loaded power, the Q–V Lissajous figures remain parallelogrammic, but the slope of line B–C and loop area increase. In Fig. 8(b) the $C_{\rm eff}$ increases with the increase of load power when the power is below 40 W. Under low load power, the number of micro-discharge channels is small, so the area of $C_{\rm eff}$, which is determined by the plasma coverage area, is smaller than that of high load power. Because $C_{\rm eff}$ is proportional to the area of $C_{\rm eff}$, $C_{\rm eff}$ changes with the number of micro-discharge channels. When the load power reaches up to 40 W, $C_{\rm eff}$ remains almost unchanged, which indicates that the number of micro-discharge channels is relatively stable at higher load power. With the power increasing, the C_0 has no obvious change, while energy per cycle ascends obviously.

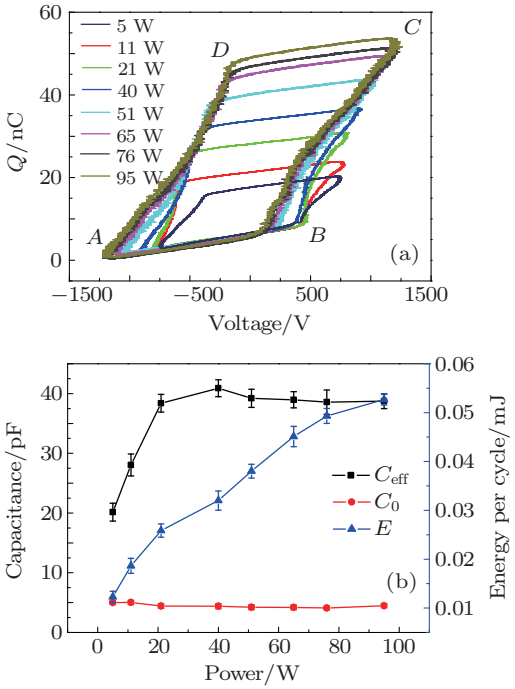


Fig. 8. (color online) Lissajous figures of RF discharge under different load powers: (a) Q–V Lissajous figures at different load powers, (b) capacitance and energy per cycle at different load powers. Other parameters are frequency: 0.67 MHz, operating pressure: 30 kPa, duty cycle: 1:20.

3.2. Emission characteristics

As a real-time and non-intrusive diagnostic method which is effective in distinguishing spatio-temporal influence, optical emission spectroscopy is widely used to investigate non-equilibrium plasma.[17–19] In this paper, the optical emission spectrum of RF SDBD plasma is measured under varying operating pressures, duty cycles and load powers.

3.2.1. Influence of operating pressure on optical emission characteristics

In this subsection, the influence of operating pressure (0.8 kPa–100 kPa) on RF SDBD plasma is investigated when the experimental conditions are as follows: the frequency of the RF generator is 0.67 MHz, the duty cycle is 1:20, and the power is 95 W. The integration time of the spectrograph is set to be 1000 ms and the actuator is placed in the pressurized chamber. The optical emission spectrogram under varying pressures is shown in Fig. 9. The optical emission spectrum plot between 300 nm and 450 nm is studied, and the emission intensity is normalized with the spectral line intensity of 380.5 nm.

Figure 10 shows the relative intensities at different operating pressures with duty cycles of 1:5, 1:10, and 1:20. The plots of relative intensity $I_{391.4}^{peak}/I_{380.5}^{peak}$ which indicates electron temperature,[4,21,22] versus operating pressure are shown in Fig. 10(a). With the pressure decreasing from 100 kPa to 4 kPa, each curve of $I_{391.4}^{peak}/I_{380.5}^{peak}$ has no obvious change. But when the operating pressure is below 4 kPa, each relative intensity increases remarkably with the decrease of operating pressure. This indicates that a transition of the RF discharge mode from filamentary discharge to glow discharge occurs at around 4 kPa, which is in accordance with Wu *et al.*'s result on the SDBD plasma driven by an AC power supply in dozens of kHz[23] and also with Choi *et al.*'s conclusion on the volumetric DBD plasma.[24] The relative intensity of $I_{371.1}^{peak}/I_{380.5}^{peak}$, which represents vibrational temperature and electron density,[4,21,22] is almost unchanged as the operating pressure varies. The trends of the relative intensities are similar to those in the cases with duty cycles of 1:5, 1:10, and 1:20.

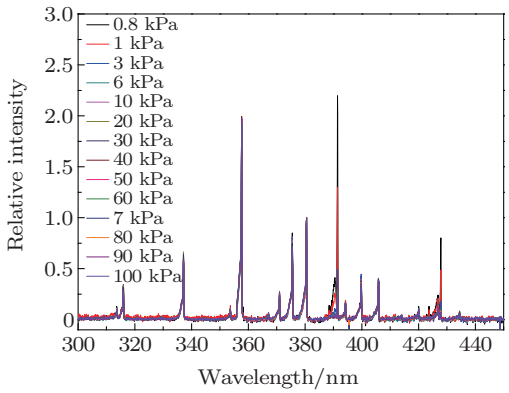


Fig. 9. (color online) Optical emission spectrogram under varying pressure.

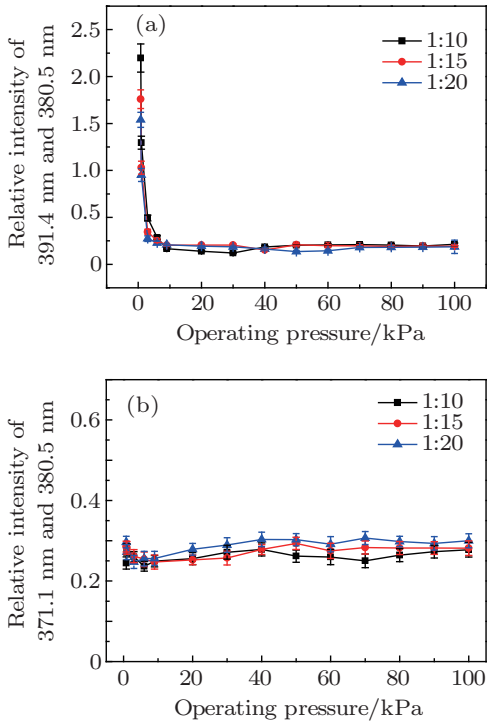


Fig. 10. (color online) Plots of relative intensity versus operating pressure with duty cycles of 1:5, 1:10, and 1:20. (a) $I_{391.4}^{peak}/I_{380.5}^{peak}$, (b) $I_{371.1}^{peak}/I_{380.5}^{peak}$.

3.2.2. Influence of duty cycle on optical emission characteristics

In Fig. 11, the optical emission spectrogram is measured under different RF generator duty cycles, which is modulated

from 1:5 to 1:20, while the integration time of the spectrograph is set to be 1000 ms. The experimental conditions are as follows: the load power is 95 W and operating pressure is 50 kPa. Figure 11(a) shows the optical emission spectrogram under varying duty cycles. It is seen in Fig. 11(b) that the relative intensities $I_{391.4}^{peak}/I_{380.5}^{peak}$ and $I_{371.1}^{peak}/I_{380.5}^{peak}$ hardly change with duty cycle, which indicates that duty cycle has no distinct influence on emission characteristics. The modulation of the RF generator can change pulse width, with the pulse period in burst mode fixed, but the relative photon of RF discharge plasma remains almost unchanged when the duty cycle decreases. The spectrum is essentially the integration of the photon over different wavelengths; when frequency and voltage each are fixed to be a certain value, discharges are the same, showing that the duty cycle has no effect on optical emission characteristics.

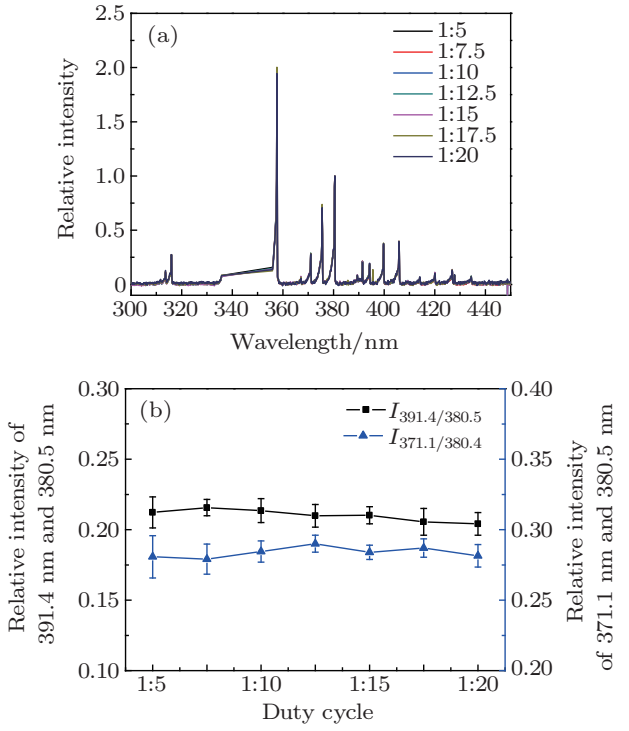


Fig. 11. (color online) Influence of the duty cycle on the optical emission spectrogram. (a) Optical emission spectrogram under varying duty cycles, (b) relative intensities under varying duty cycles.

3.2.3. Influence of load power on optical emission characteristics

Figure 12 shows the influences of load power (5 W–95 W) on RF discharge plasma, when the experimental conditions are as follows: the frequency of the RF generator is 0.67 MHz, the duty cycle is 1:20, the pressure is 30 kPa, and the integration time of the spectrograph is 1000 ms. The optical emission spectrogram under varying load powers is shown in Fig. 12(a), and two lines are plotted in Fig. 12 to analyze the relative intensity. The relative intensity $I_{391.4}^{peak}/I_{380.5}^{peak}$ rises with the increase of load power, and this conclusion is interesting and worthy of further research. On the contrary, no obvious variation of relative intensity $I_{371.1}^{peak}/I_{380.5}^{peak}$ can be found under different load powers.

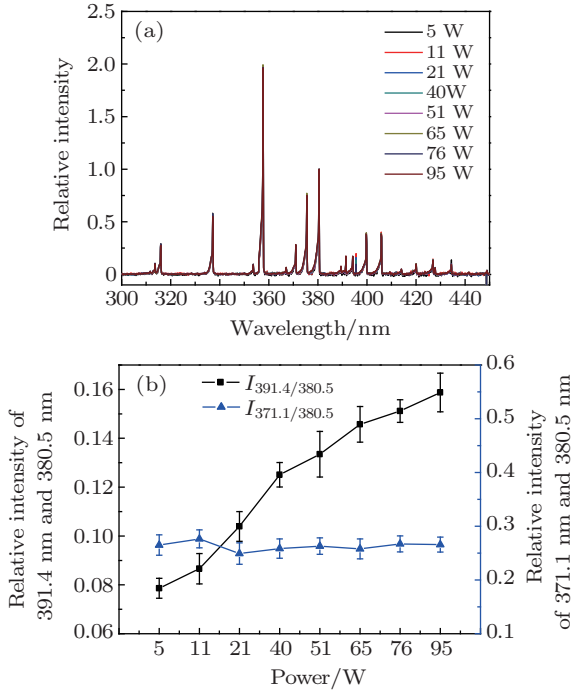


Fig. 12. (color online) Influences of load power on the optical emission spectrogram. (a) Optical emission spectrogram under varying load power, (b) relative intensities under varying load power.

4. Conclusions

The electrical characteristics and optical emission spectra of RF SDBD plasma under varying operating pressures, duty cycles, and load powers are experimentally investigated. The main conclusions are as follows.

The current waveform of RF SDBD has two obvious peaks at low pressure, while it possesses many spikes when operating pressure is relatively high. At a low operating pressure, the discharge mode is homogeneous and diffuses glow discharge. *Q*–*V* Lissajous figures of RF SDBD each are like a parallelogram under different operating pressures. The peak-to-peak value of the voltage ascends when the operating pressure is relatively high. When the operating pressure reaches up to 30 kPa, C_{eff} decreases remarkably while energy per cycle increases rapidly with the increase of pressure. *Q*–*V* loops, capacities, and energies per cycle remain almost unchanged under different duty cycles. When the load power is below 40 W, C_{eff} increases with the increase of load power, but it remains almost unchanged with load power in a range between 40 W and 95 W, which indicates that the discharge current is relatively stable during this period. The energy per cycle rises as load power increases.

When the duty cycle and load power of the RF power are fixed, with the pressure decreasing from 100 kPa to 4 kPa, the relative intensity $I_{391.4}^{peak}/I_{380.5}^{peak}$ has no obvious change. When the operating pressure is below 4 kPa, $I_{391.4}^{peak}/I_{380.5}^{peak}$ increases

sharply with the decrease of operating pressure, which indicates that the RF discharge mode transforms from filamentary discharge to glow discharge at around 4 kPa. Relative intensity $I_{371.1}^{\text{peak}}/I_{380.5}^{\text{peak}}$ is approximately the same when pressure varies from 0.8 kPa to 100 kPa. There is no distinct influence of the duty cycle on the emission characteristics. When experimental conditions are fixed except for load power, with the increase of power, $I_{391.4}^{\text{peak}}/I_{380.5}^{\text{peak}}$ tends to ascend obviously, while $I_{371.1}^{\text{peak}}/I_{380.5}^{\text{peak}}$ hardly changes.

The future work should focus on the characteristics and control of RF discharge in a high speed flow, and RF DBD plasma on shockwave control, and provide new technical solutions for enhancing flow control ability.

References

[1] Roth J R 2003 *Phys. Plasmas* **10** 2117
[2] Patel M P, Ng T T and Vasudevan S 2007 *J. Aircraft* **44** 1264
[3] Li Y H, Wu Y, Zhu J Q, Zhou M, Su C B, Zhang X W and Zhu J Q 2010 *Exp. Fluids* **48** 1015
[4] Wu Y, Li Y H, Jia M, Song H M, Su C B and Pu Y K 2010 *Chin. J. Aeronautics* **23** 39
[5] Shao T, Jiang H, Zhang C, Yan P, Lomaev M I and Tarasenko V F 2013 *Europhys. Lett.* **101** 45002
[6] Jiang H, Shao T, Zhang C, Li W F, Yan P, Che X K and Schamiloglu E 2013 *IEEE Trans. Dielectr. Electr. Insul.* **20** 1101
[7] Dedrick J, Boswell R W, Audier P, Rabat H, Hong D and Charles C 2011 *J. Phys. D: Appl. Phys.* **44** 205202
[8] Leonov S, Bityurin V, Klimov A, Kolesnichenko Y and Yuriev A 2001 32*th AIAA Plasmadynamics and Lasers Conference*, June 11–14, 2001, Anaheim, SUA, p. 3057
[9] Leonov S and Yarantsev D A 2008 *J. Propul. Power* **24** 1168
[10] Moralev I, Klimov A, Bityurin V and Kazansky P 2014 52*nd Aerospace Sciences Meeting*, January 13–17, 2014, National Harbor, USA, p. 1263
[11] Klimov A, Bitiurin V, Moralev I, Tolkunov B and Kasansky P 2010 48*th AIAA Aerospace Sciences Meeting*, January 4–7, 2010, Orlando, USA, p. 782
[12] Dedrick J, Im S, Cappelli M, Boswell R W and Charles C 2013 *IEEE Trans. Plasma Sci.* **41** 3275
[13] Manley T C 1943 *Trans. Electrochem. Soc.* **84** 83
[14] Kettlitz M, Höft H, Hoder T, Reuter S, Weltmann K D and Brandenburg R 2012 *J. Phys. D: Appl. Phys.* **45** 245201
[15] Kriegseis J, Möller B, Grundmann S and Tropea C 2011 *J. Electrostat.* **69** 302
[16] Grundmann S and Tropea C 2009 *Int. J. Heat Fluid Flow* **30** 394
[17] Kim D B, Rhee J K, Moon S Y and Choe W 2006 *Appl. Phys. Lett.* **89** 061502
[18] Enloe C L, McLaughlin T E, VanDyken R D, Kachner K D, Jumper E J and Corke T C 2004 *AIAA J.* **42** 589
[19] Borghi C A, Cristofolini A, Carraro M R and Neretti G 2006 37*th AIAA Plasmadynamics and Lasers Conference*, June 5–8, 2006, San Francisco, USA, p. 3380
[20] Fantz U 2006 *Plasma Sources Sci. Technol.* **15** 137
[21] Zhu X M and Pu Y K 2005 *Phys. Plasmas* **12** 103501
[22] Zhu X M and Pu Y K 2006 *Phys. Plasmas* **13** 063507
[23] Wu Y, Li Y G, Jia M, Song H M, Guo Z G, Zhu X M and Pu Y K 2008 *Appl. Phys. Lett.* **93** 031503
[24] Choi J H, Lee T I, Han I, Baik H K, Song, K M, Lim Y S and Lee E S 2006 *Plasma Sources Sci. Technol.* **15** 416